EFFICACY OF ZINC SULFIDE- CHITOSAN NANOPARTICLES AGAINST BACTERIAL DIABETIC WOUND INFECTION

Mustafa H.N. **I. Al -Ogaidi**
Researcher **Assist. Prof.**
Department of Biotechnology, College of Science, University of Baghdad, Baghdad, Iraq.
mustafa87hatem@yahoo.com **biotechphd2011@yahoo.com**

ABSTRACT

This study was aimed evaluation, Zinc sulfide-chitosan nanoparticles (ZnS-chitosan NPs) as an antibacterial agent. The nanoparticles of Zinc sulfide-chitosan were synthesized using a single-step colloidal process. Different factors were optimized, which included pH, temperature, reaction time, concentrations of chitosan and Zinc chloride .The optimal conditions was achieved at pH 7, temperature 60℃, reaction time 60min, with 0.04 mg/ml of Zinc chloride, 2.5 ml 0.1mg/ml Sodium sulfide and 0.009 M chitosan. The size of ZnS-chitosan NPs size was tested by using FESEM which were 35nm, surface morphology was done by using AFM. Moreover, X-ray Diffraction (XRD) characterized the crystal structure. While the nature of functional groups present in ZnS-chitosan nanoparticles was determined by Fourier transforms infrared (FT-IR) analysis. The sensitivity of bacterial isolates to antibiotics were tested, the bacteria were more sensitive, resistant, and moderate range to ten antibiotics. Different concentrations (12.5, 25, 50, 100, 200, and 400 µg/ml) of ZnS-chitosan NPs were investigated against multidrug resistance (MDR) *Staphylococcus aureus* (Gram-positive bacteria) and *Acinetobacter baumannii*, *Pseudomonas aeruginosa* (Gram-negative bacteria). The minimum inhibitory concentration of ZnS-chitosan NPs against pathogenic bacteria was 100 µg /ml *for Staphylococcus aureus* and *Acinetobacter baumannii*, while 50 µg /ml for *Pseudomonas aeruginosa*. Cytotoxicity effects of ZnS-chitosan on normal cell lines (WRL-68) were investigated by MTT assay. The results showed that the ZnS-chitosan nanoparticles no cytotoxic effect on normal cell line.

Key words: zinc sulfide nanoparticles, chitosan, cytotoxicity, antibacterial

تقييم فعالية دقائق كبريتيد الزنك الكيتوسان النانوية ضد البكتريا المسببة لالتهابات القدم السكري

مصطفى حاتم نافع اسراء علي زيدان
باحث أستاذ مساعد
قسم التقنيات الاحيائية – كلية العلوم – جامعة بغداد، بغداد، العراق

المستخلص

من الهدف الدراسة، تقييم دقائق كبريتيد الزنك والكيتوسان النانوية (ZnS–chitosan NPs) كعامل مضاد للبكتيريا. تم تصنيع الدقائق النانوية لكبريتيد الزنك باستخدام عملية غروانية من خطوة واحدة. تم تحسين العوامل المختلفة، والتي تضمنت درجة الحموضة ودرجة الحرارة ووقت التفاعل وتركيزات الكيتوسان وكلوريد الزنك. تم تحقيق الظروف المثلى عند الأس الهيدروجيني 7 ودرجة الحرارة 60 درجة مئوية ووقت التفاعل 60 دقيقة مع 4 مل 0.009 مولار من كلوريد الزنك و 2.5 مل 0.1 مجم / مل من كبريتيد الصوديوم و 0.009 مولار من الشيتوزان. تم اختبار حجم ZnS–chitosan NPs باستخدام FESEM الذي كان 35 نانومتر ، وتم إجراء التشكل السطحي باستخدام AFM. علاوة على ذلك ، يتميز حيود الأشعة السينية (XRD) بالبنية البلورية. بينما تم تحديد طبيعة المجموعات الوظيفية الموجودة في الجسيمات النانوية ZnS–chitosan بواسطة تحليل فورييه لتحويلات الأشعة تحت الحمراء (FT–IR). تم اختبار حساسية العزلات البكتيرية للمضادات الحيوية وكانت البكتريا أكثر حساسية ومقاومة ومتوسطة المدى حتى عشرة مضادات حيوية. تم فحص تراكيز مختلفة (12.5 و 25 و 50 و 100 و 200 و 400 ميكروغرام / مل) من ZnS–chitosan NPs ضد مقاومة الأدوية المتعددة (MDR)(*Staphylococcus aureus*) (بكتيريا موجبة الجرام) (*Acinetobacter baumannii*) و (*Pseudomonas aeruginosa*) (سالبة الجرام) بكتيريا). كان الحد الأدنى للتركيز المثبط لـ ZnS–chitosan NPs ضد البكتيريا المسببة للأمراض 100 ميكروغرام/ مل للمكورات العنقودية الذهبية و (*Acinetobacter baumannii*) ، بينما 50 ميكروغرام / مل لـ (*Pseudomonas aeruginosa*). تم فحص تأثيرات السمية الخلوية لـ ZnS–chitosan على خطوط الخلايا الطبيعية (WRL–68) بواسطة مقايسة MTT. أظهرت النتائج أن الجسيمات النانوية ZnS–chitosan ليس لها تأثير سام للخلايا على خط الخلية الطبيعي.

الكلمات المفتاحية: دقائق كبريتيد الزنك النانوية، الكيتوسان، السمية الخلوية،فعالية ضد بكتيرية.

Received:15/4/2021, Accepted:22/7/2021

INTRODUCTION

Wound injuries are part of the most common and serious types of trauma, representing Major public health concern, and wound healing is a complex process with many potential factors that can delay healing (63). Wound infection is a localized defect or excavation of the skin or underlying soft tissue in which pathogenic organisms have invaded into viable tissue surrounding the wound (45). 1-4 Bacterial wound infections are caused by antimicrobial-resistant bacteria and are related to increased morbidity and health costs. (47). It is a major cause of morbidity and mortality in developing countries (57). 5-7 Patients with wounds are more vulnerable to infection due to the loss of the normal protective skin barrier (15). Diabetic foot ulcers are a major worldwide healthcare problem that is increasing at an alarming rate; possibly, because of the double-digit increase in diabetes each year increased longevity, and patients having diabetes for longer periods of time. (43). Common bacterial pathogens associated with wound infection include *Staphylococcus aureus, Escherichia coli, Pseudomonas aeruginosa, Klebsiella pneumonia, Streptococcus pyogenes, Proteus spp., Streptococcus spp., and Enterococcus spp*. (59). These species are naturally resistant to certain antibiotics and antiseptics and are able to populate injured skin even in the scarcity of enough nutrients (46). In recent decades, there has been a great deal of scientific activity in nanotechnology. Several techniques, such as physical or chemical methods, have been used in various fields of science for the construction of nanoscale materials (5). Polymer composites could have better physical properties if the current content mixture can be manufactured to satisfy special specifications that are hard to achieve with the use of single components (20). Zinc sulphide (ZnS) is an essential material of the semiconductor to the II-VI group which is a leading candidate for various sensing and optoelectronic devices (8). ZnS has two different allotropic forms - zinc blend or sphalerite (cubic) and wurtzite (hexagonal close pack) among which the cubic form has a more stable phase at low temperatures (64). Zinc sulfide (ZnS) nanoparticles have the potential to applications as antibacterial agent (24). Chitosan is an N-acetyl glucosamine polymer and can be gained by chitin deacetylation, It consists of alternating units of (1 - 4) connected N-acetyl glucosamine and glucosamine (71). Cuticles of various crustaceans, mostly crabs, shrimps, and insect exoskeletons, are the main source of raw materials for chitin extraction (72). The most significant biological activities of chitosan include its antimicrobial, antiviral, antitumor, and antioxidant properties (38). They are also antihypertensive, anticoagulant, anti-allergic, anti-inflammatory, anticancer, anti-inflammatory, and mucoadhesive (73). These characteristics are especially suited to a wide variety of therapeutic and pharmaceutical uses, including wound healing (23). Gene delivery (49). In addition, drug delivery (60). Chitosan has a broad range of antimicrobial activity against both gram-positive and gram-negative bacteria, with a large degree of destruction caused by chitosan and its derivative products interacting with the bacterial cell wall (40). This study aimed to synthesize zinc sulfide-chitosan Nps by single step method, characterize the synthesized NPs, and evaluate their bacteria activities against multi-drug resistance bacteria isolated from diabetic wound infection cases.

MATERIAIS AND METHODS

Zinc chloride ($ZnCl_2$), sodium sulfide (Na_2S $9H_2O$), sodium hydroxide (NaOH), acetic acid (CH_3COOH), and hydrochloric acid (HCl), were used as minification recombinant. Chitosan powder (at 1% in 1% acetic acid) was used as the reference ligand, Deionized water (DI-water).

Samples collection

Fifty-one from diabetic foot infection samples including 12 isolates of *staphylococcus aureus*, 11 isolates of *pseudomonas aeruginosa*, and 9 isolates of *Acinetobacter baumannii*, *E. coli* 5, *Klebsiella p* 5, *s.epidermids* 3, *Proteus mirabils* 2, *S. haemolyticus* 2, *and serratia spp* 2 was randomly selected from people who had a wound infection. During the months from September to December 2020, samples were obtained from participants of both sexes at various hospitals in Baghdad, including the Medical City and Al-Wasity hospital. Samples

were collected in sterile environments and transported to the lab within 1-2 hours.

Isolation and identification of bacteria

The identification of bacterial isolates was done by standard biochemical tests on the isolates and these include morphological, gram stain and cultural characteristics of colonies on blood agar MacConkey agar, and Mannitol Salt Agar, also hemolysis, production of oxidase, and catalase, were done to confirm pathogenic staphylococci. Further tests carried out for gram-negative microorganisms including indole test, methyl red test, vogas-proskaure test, simmons citrate test and lactose fermentation test. The detection of the isolates was also verified by BioMérieux's Vitek 2 portable auto-analyzing method.

Antibiotic susceptibility test

The Clinical and Laboratory Standards Institute (CLSI2020) recommendations (14) were used to conduct susceptibility experiments on bacterial isolates using an updated Kirby-disk Bauer's diffusion system (27). One to three colonies of bacteria isolates were grown overnight on Müller-Hinton agar at 37°C for 24 hours at the optimum incubation temperature Bacterial cultures were standardized to meet 0.5 McFarland specifications, and the bacterial suspension was streaked onto Müller-Hinton agar using a sterile swab. The isolates were graded as responsive (S) or resistant (R) according to the CLSI guidelines (2020). The following antibiotics were tested: Amikacin (AK), Cefotaime (CTX), Ciprofloxacin (CIP), Trimethoprim (TMP), Levofloxacin (LEV), Vancomycin (Va), Impenem (IPM), Tetracycline (TE) ,Aztreonam (ATM), and Piperacillin (PRL). All the antibiotics used in this study were purchased from Himedia, India.

Tetrazolium Cytotoxicity (MTT) Assay

In accordance with the Manufacturer's Instructions (MTT Kit/Intron Biotech, Korea), both the planning of the solution and experimental tests were carried out. 1 x 10^4 cell/ml is cultivated in 96-well plates and the volume with RPMI medium was filled up to 200 micro liter for every well. The panels were moved gently, sterile topped, and incubated at a concentration of 5 percent CO2 for 24 hours at 37°C. The medium and 200µl ZnS-chitosan NPs were then separated. The medium is isolated from the wells and 200µL (12.5, 25, 50, 100, 200, and 400) µg/ml of ZnS-chitosan NP are used. In addition to the others, three replicates of every regulation and concentration process have been performed with each experimental replicate containing positive control (doxorubicin 50 mg/mL) and adverse control (DMSO). The flat was replenished with 5 percent CO2 at 37°C over 48 hours. After the ZnS-chitosan NPs treatment, a solution of 10ml of MTT was added to each well and four hours were reincubated at 37° C, 5% CO2. 100µl of DMSO solution was added to each well and incubated for five minutes after removal of the medium. The viability of the cells was measured using the optical intensity at a wavelength of 575 nm absorbance and the following formula:

Cell Viability% = Optical density of sample x 100%
The optical density of the control

Preparation of Zinc sulfide-chitosan nanoparticle: Preparation of Zinc Sulfide-chitosan nanoparticles was performed using a single-step aqueous colloidal process by (53).With some modifications, including optimization (temperature, time, PH, and concentration of Chitosan, Zinc chloride, and sodium sulfide). Chitosan solution was prepared by dissolving 0.009 M of chitosan in 2 ml Acetic acid in 97 ml distal water. 4 ml 0.04 mg/ml Zinc chloride and 2.5 ml 0.1mg/ml of Sodium sulfide. Steps for ZnS-chitosan nanoparticle preparation are described below: The first step: 4 ml was dropped from chitosan stock and then added slowly to 4 ml of zinc chloride stock solution and 2.5 ml of Sodium sulfide. The second step: mix was exposed to regular stirring for 90 minutes. The third step: wish the solution by D.W.

Optimized conditions for ZnS-chitosan Nps synthesis

The effect of Ph: The ZnS-chitosan colloidal were prepared with different pH, the pH was adjusted using HCL (0.1N) to test different pH value, which was (5, 7, 9, 11). And NaOH (0.1N). The absorption of the resulting solutions was measured using a Uv-vis spectrophotometer.

The effect of temperature

The ZnS-chitosan colloidal were prepared with different pH, that adjusted using HCL (0.1N)

to test different pH value, which was (5, 7, 9, 11).and NaOH (0.1N). The absorption of the resulting solutions was measured using a Uv-vis spectrophotometer.

The effect of reaction time

The ZnS-chitosan nanoparticles (ZnS-chitosan NPs) were prepared at different temperature (30, 40, 50 and 60℃), using a stirring hot plate to fix the suitable temperature. The absorbance of the resulting solutions was measured by using Uv-Vis spectrophotometrically

The effect of Concentrations

The present study used different concentrations of chitosan, Zinc chloride, and Sodium sulfide in order to prepare zinc sulfide-chitosan nanoparticles. These concentrations are listed in the Table **1**

Table 1. Different Concentration in ZnS-CH NPs Formulations

Formulation	Chitosan	Zinc chloride	Sodium sulfide	References
Formula 1	0.0065M	4 ml 0.008 mg/ml	2.5 ml 0.01mg/ml	(53)
Formula 2	0.009M	4 ml 0.04 mg/ml	2.5 ml 0.1mg/ml	Modified method (53)

Characterization of the prepared nanoparticles: Atomic Force Microscopy (AFM) was used to create a three-dimensional surface topography, with measurements based on van der Waals or other enticing and repulsive forces on a glass slide, five drops of ZnS-chitosan nanoparticles were applied and allowed to dry and precipitate. Another characterization technique such as UV/Visible spectroscopy is a technique used to quantify the light that is absorbed and scattered by a sample (a quantity known as the extinction, which is defined as the sum of absorbed and scattered light), X-Ray Diffraction was used to achieve important features such as crystal structure and height, Field emission scanning electron microscopy (FESEM) provides topographical and elemental information at magnifications of 10x to 300,000x, with virtually unlimited depth of field, and Zeta potential is the measurement of the electric potential at the interface of the electrical double layer, Zeta potential is the potential at the hydrodynamic shear plane and can be determined from the particle mobility under an applied electric field (39).

Antibacterial activity of Zinc Sulfide-Chitosan nanoparticles: ZnS-chitosan nanoparticles were analyzed with gram-negative bacteria (*Acinetobacter baumannii, Pseudomonas aeruginosa*) and gram-positive bacteria that were isolated from contaminated sores (*Staphylococcus aureus*). A broth micro dilution test was used to evaluate the minimum inhibitory concentration (MIC) of ZnS-chitosans Nanoparticles. In each sterile sterilizer channel, a ratio of 1:1 diluted, the ZnS-chitosan nanoparticles were applied from each concentration to 500 µL of double Muller-Hinton broth at a difference in concentration (12,5, 25, 50, 100, 200, and 400 µg/ml). Following shaking, each tube was then added with 500 µL of diluted nanoparticles. The microbial suspensions of 0.5 MacFarland were modified and diluted to 1 to 10^6 CFU/mL, then 50 µL of the suspension was applied to every tube, and incubated at 37 ± 2 °C for 24 hours. The suspension was diluted in a single rod. MIC levels were reported to inhibit bacteria after 24 hours as the lowest compound concentration (50).

RESULTS AND DISCUSSION

Isolation and identification of bacterial isolates: The VITEC2 compact device was used to confirm the diagnosis of all bacteria isolates after identified macroscopically, morphologically by culture media and several bio chemical test table 2. Among the isolates were *Staphylococcus aureus* (23.52%) (3). whereas the value was (21.56%) for *pseudomonas aeruginosa* (2). (17.64) for *Acinetobacter baumannii* (9). (9.80%) for *Klebsiella p* (41). (9.80%) for *E. Coli* (11). (5.88%) for s.epidermids (67).(3.92%) for *serratia marcescens* (17). (3.92%) for *S. haemolyticus* (44). In addition (3.92%) for *Proteus mirabilis* (65). The proportion of each bacterial isolate to the total isolates and Percentage frequency of bacterial isolates from diabetic wound infection are presented in table 3.

Antibiotic sensitivity

Most isolates are presented multidrug tolerance profiles; 100% of isolates were resistant to trimethoprim, ciprofloxacin, and clindamycin, with a high degree of resistance

to Levofloxacin 99.6 %. Additionally, they exhibited roughly tolerance to cefotaxime and amikacin, with rates of resistance of 61.1 percent and 58.1 percent, respectively. Each bacterial isolate exhibited a high rate of Carbapenem resistance. In general, three pathways contribute to resistance to Carbapenem (a) Hydrolysis sensitive to plasmid AmpCs and ESBL enzymes; contribute to carbapenem agents' insensitive (b) Transfer of ESBL genes between the organisms (70). and (c) porin mutation with expression modulation (13). Bacterial isolates that showed resistance to Vancomycin, Aztreonam, Impineim, represented an appropriate option for the part of this work, in table 4

Optimization for synthesis ZnS-chitosan nanoparticles: Different factors for optimizing the synthesis of ZnS-chitosan nanoparticles such as (pH, temperature, time and concentration of chitosan 0.009 M, 0.04 mg/ml Zinc chloride and 0.1mg/ml of Sodium sulfide.) were investigated in this study. PH has a significant effect on nanoparticle formation and has the capability of influencing compounds that used in the mixture by a charge change. At high pH, the nanoparticles started to agglomerate and particles suffer from aggregation (54). Temperature rise will increase the reaction rate and synthesis efficiency. Most experiments are performed at room temperature, as it is the simplest and natural way to synthesize the nanoparticles. When the temperature increases, the reaction time decreases, and 95 % is transformed to nanoparticles within a short period (37). Increasing temperature lead to anxiety in the reaction and increase the probability of aggregation, therefore the particle size increased with increasing temperature. Time is one of the major parameters affecting nanoparticle synthesis directly. Nevertheless, it is shown that particle size decreases with increasing time, and at a given time, it stabilizes. The optimum pH for ZnS-chitosan NPs (5, 7, 9, and 11) was (7.0), and the time (60 min), these results were in agreement with (4). Moreover, the temperature at (60 ° C), these results were in agreement with (6).

Table 2. Biochemical tests of. Isolated from diabetic wound infection

	Biochemical test						
Bacterial isolates	**Catalase**	**Oxidase**	**Indole**	**Methyl Red**	**Voges Proskaur**	**Simmons Citrate**	**Lactose fermentation**
Staphylococcus aureus	+	-	/	/	+	+	+
Pseudomonas aeruginosa	+	+	+	+	+	-	-
Acinetobacter baumannii	+	-	-	-	-	+	-
Klebsiella pneumonia	+	-	-	-	+	+	+
Escherichia coli	+	-	+	+	-	-	+
Staphylococcus epidermids	+	-	/	/	+	+	+
Serratia marcescens	-	/	+	+	-	+	+
Staphylococcus haemolyticus	+	-	/	/	+	+	+
Proteus mirabilis	+	-	-	+	-	+	-

Table 3. Distribution and frequency of bacterial isolated from diabetic wound infection

Bacterial isolates	Frequency	Percentage
Staphylococcus aureus	**12**	**23.52%**
Pseudomonas aeruginosa	**11**	**21.56%**
Acinetobacter baumannii	**9**	**17.64%**
Klebsiella pneumonia	**5**	**9.80%**
Escherichia coli	**5**	**9.80%**
Staphylococcus epidermids	**3**	**5.88%**
Serratia marcescens	**2**	**3.92%**
Staphylococcus haemolyticus	**2**	**3.92%**
Proteus mirabilis	***2***	**3.92%**

Table 4. percentage of antimicrobial susceptibility of bacteria isolated from diabetic wound infection

bacterial isolates	N0. Of Isolates resistant (%)									
	CIP	AK	TE	VA	LEV	IMP	CTX	PRL	ATM	TMP
Staphylococcus aureus	25%	21%	0%	8%	17%	0%	5%	6%	0%	6%
Pseudomonas aeruginosa	18%	9%	9%	0%	27%	0%	0%	27%	9%	70%
A. baumannii	0%	0%	0%	25%	0%	30%	10%	10%	20%	2%
E. coli	28%	14%	0%	8%	17%	0%	6%	6%	28%	50%
Klebsiella p	20%	20%	0%	0%	10%	0%	30%	0%	0%	60%
Proteus mirabils	33%	33%	0%	0%	11%	0%	6%	56%	44%	44%
Serratia marcescens	50%	50%	50%	0%	20%	0%	25%	0%	0%	75%
s.epidermids	20%	20%	0%	0%	10%	0%	20%	0%	0%	60%
S. haemolyticus	50%	50%	0%	0%	10%	0%	50%	0%	0%	100%

Characterization of ZnS-chitosan NPs: The optical characteristics of the nanoparticles were studied using UV – Visible spectrometer. Figure (1) shows the absorbance of the sample in the Nano range. It has shown a peak at 393 nm wavelength was thus similar to the absorption spectra 417 nm these results were in agreement with by (69).In addition, the absorbance peak to ZnS nanoparticles was recorded at 469 nm in Figure (2). Thus similar to the absorption spectra 314 nm result by (33).The two figures demonstrated that the shape of spectra became broad and the position of peak was shifted after coating with chitosan that can improve the presence of chitosan.

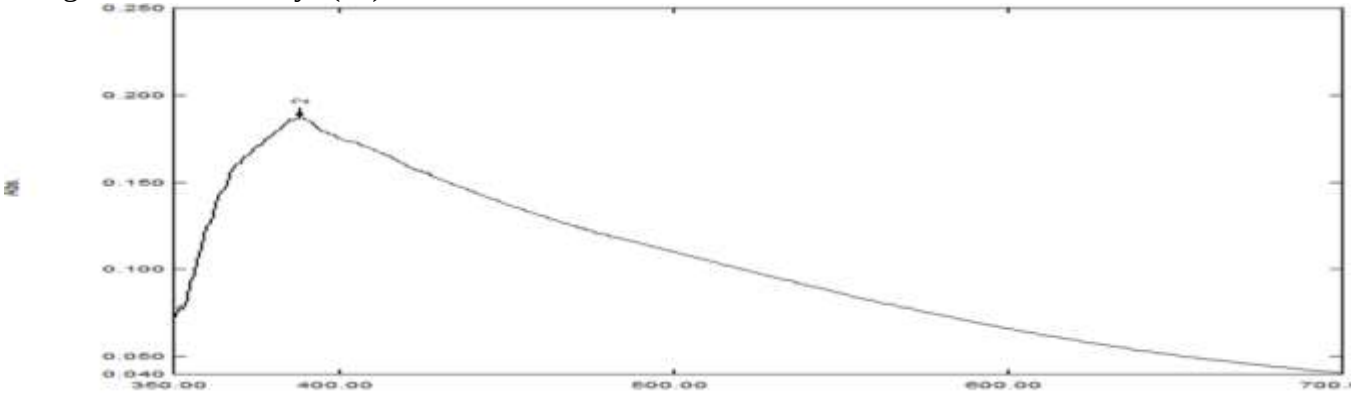

Figure 1. absorbance peak of ZnS-chitosan nanoparticles using UV-visible spectrometer of ZnS NPs

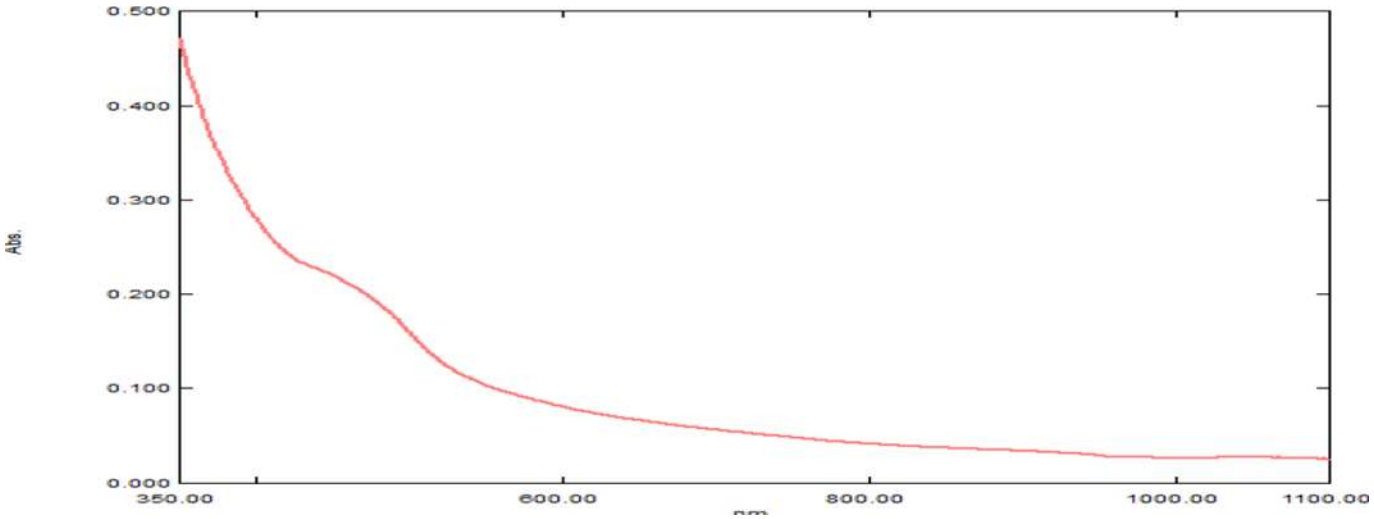

Figure 2. absorbance peak of ZnS nanoparticles using UV -visible spectrometer

Atomic force microscopy (AFM):

ZnS-chitosan and ZnS NPs were investigated with atomic force microscopy in their surface morphology, ZnS-chitosan, and ZnSNPs with 2D and 3D topology (figure3) and (figure 5). The synthesized ZnS -chitosan NPs seen in AFM images are in a spherical form and have a median diameter was 20.10 nm these results were in agreement with (10). (figure4). In addition, ZnS nanoparticles seen in AFM images are in a spherical form and have a median diameter was 18.5 nm (figure 6) these results were in agreement with (28).

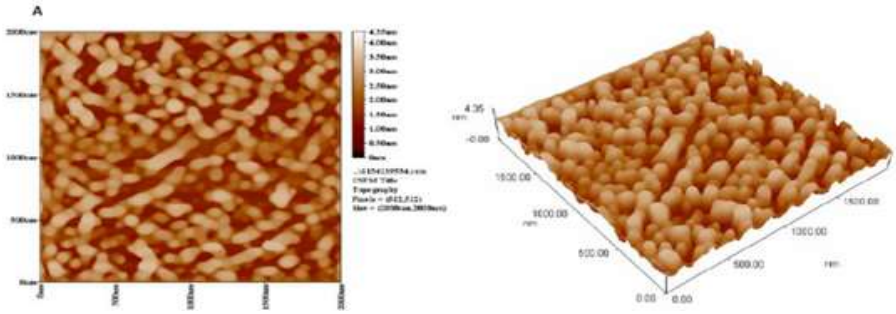

Figure 3. Atomic force microscopy of Zinc sulfide illustrate 2D and 3D topological of chitosan nanoparticles

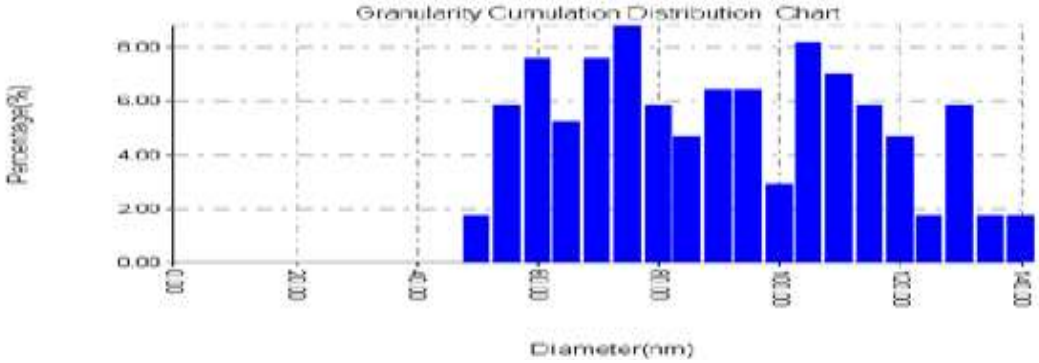

Figure 4. Average size of Zinc Sulfide nanoparticles byAFM

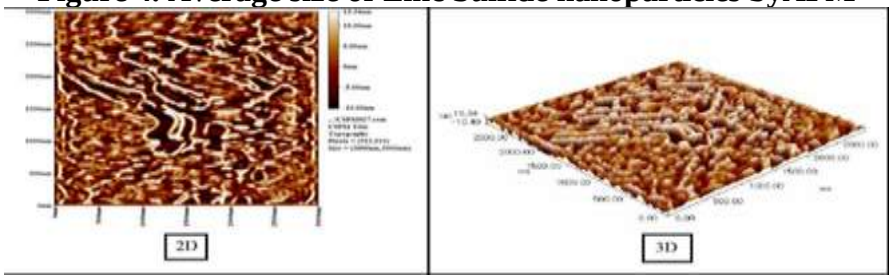

Figure 5. Atomic force microscopy of ZnS / chitosan illustrate 2D and 3D topological of chitosan nanoparticles

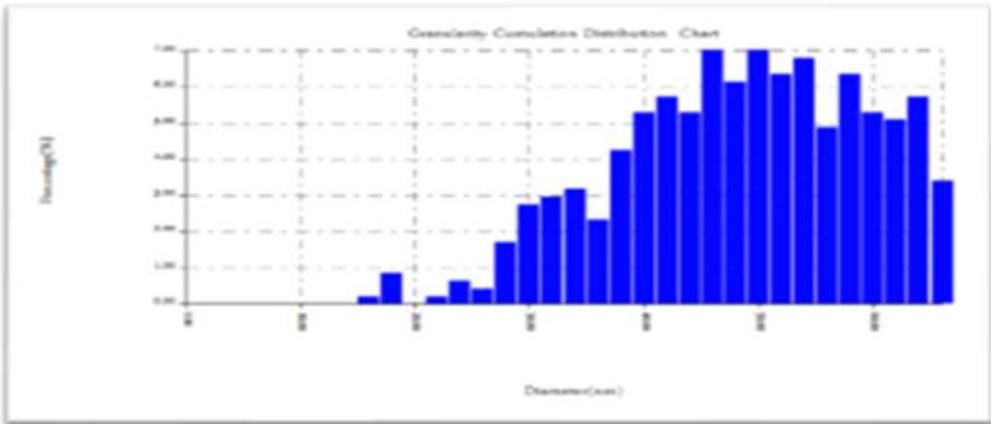

Figure 6. Average size of ZnS-chitosan nanoparticles byAFM.

X-ray Diffraction (XRD) analysis

The XRD patterns (figure 7) show the distinctive diffraction peaks of ZnS-chitosan NPs at 2θ 28.82°, 36.17°, 45.44°and 57.42° these peaks were well matched with standard Diffraction data of ZnS-chitosan NPs (JCPDS file no. 77- 2100), and attributed to the (111), (200), (220) and (1015) ZnS-chitosan NPs were found to contain the lattice parameters = 1.6277 A ° which verified the existence of cubic ZnS-chitosan, the size of the ZnS-chitosan NPs Calculated by the Debye-Scherer equation (D = 0.94λ/ cosθ). while the XRD (figure 8) shows the distinctive diffraction peaks of ZnSNPs at 2θ 27.12°, 48..19°, and 56.7° These peaks were well matched with standard diffraction data of ZnS NPs (JCPDS file no. 80-0020) and attributed to the (111), (220) and (311) Lattice parameters of ZnS NPs were found to be a =1.6277 A °, which have confirmed the presence spherical ZnS

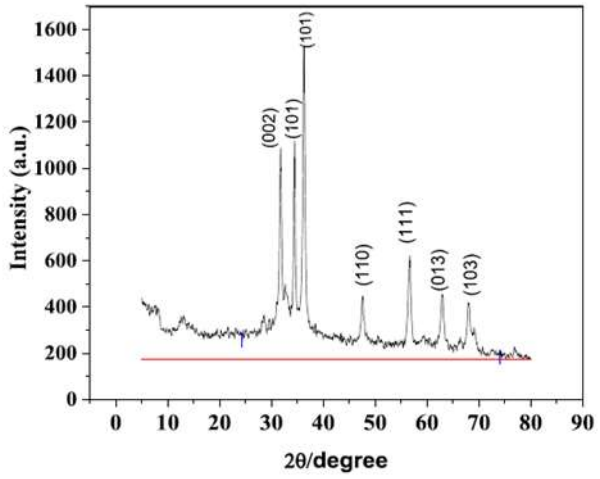

Figure 7. The XRD of ZnS-chitosan nanoparticle

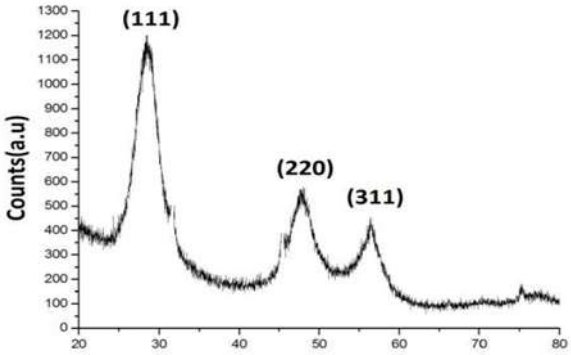

Figure 8. The XRD of ZnS-chitosan nanoparticle

Zeta potential measurement of ZnS-chitosan: The Zeta characterization method was used to characterize the stability and dispersion of ZnS-chitosan NPs. The results of the Zeta-potential measurement presented a positive charge for zeta value 61.70+ 0.80 mV reflecting the stability of the colloidal suspensions as shown in (Figure 9) (29).When the zeta potential value increases, the particles repel each other with more force, the tendency of aggregation decreases and the particles form a more stable profile (16).Moreover, this strong positive ZP means that the nanoparticles are stable under the conditions present and have a high capacity for absorption via the negatively charged cell membrane. In addition, The Zeta potential measurements of the biosynthesized ZnS NPs show in figure (10) a sharp peak at -53.2 mV indicative that the surface of the nanoparticles is negatively charged. Generally, the zeta potential of the nanoparticles should be either highest than +30 mV or lower than -30 mV (62).After the addition of ZnS nanoparticles in chitosan solution (ZnS-chitosan), the increase in the ZP to more positive values was evidenced in the entire studied pH range. This shift was caused by the properties of chitosan.

Chitosan is a cationic polymer, with pKa ~6.5, which is insoluble in water at neutral pH, at which the majority of amines from the molecule are deprotonated. On the other hand, at acidic pH, the chitosan becomes water-soluble, as it is positively charged (12). The creation of the ZnS-chitosan colloidal system brought about the increased stability of the suspension from the incipient instability area to a good stability area (up to +61.70 mV at pH 7). As was determined earlier (58).

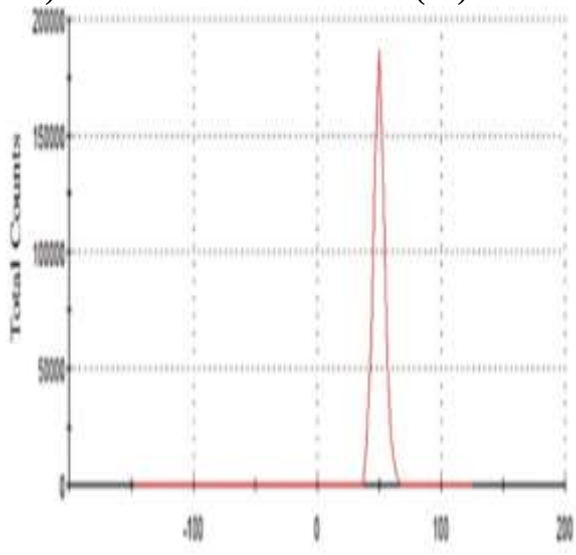

Figure 9. The Zeta potential measurement of ZnS-chitosan nanoparticle

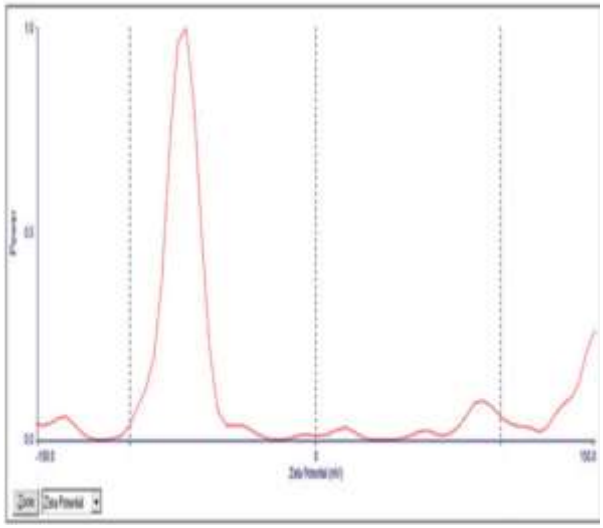

Figure 10. The Zeta Potential Measurement of ZnS nanoparticle

Field emission scanning electron microscope (FE-SEM) of Zinc sulfide chitosan nanoparticles: The FESEM measurement of the chitosan-ZnS nanocomposite in (figure11A) showed the existence of very well separated distorted Nano spherical structures of ZnS that grafted on the chitosan sheet. Through this measurement in (Figure 11A), the size of the zinc sulfide nanoparticles, which reached 35-37 nm that is less than that, found in the pure ZnS, was calculated for the ZnS nanoparticles that grafted on the surface of the chitosan-ZnS nanocomposite. The presence of chitosan in the composite structure was shown by the formation of a sheet-like nanostructure in (figure11B). The measurement clearly shows the presence of zinc sulfide nanoparticles on the surface of chitosan. The presence of this composition is conclusive evidence of the success of the reaction and the stabilization of zinc sulfide on the surface of chitosan. The unified distribution of zinc sulfide particles and their distribution around the surface of discrete, non-aggregated particles is a remarkable accomplishment for a Nano construction where such a distribution is considered an optimum distribution of the material; these results were supported by (26).(figure 12) FESEM images were measured and topographical analysis was performed based upon the surface study. Synthesized ZnS NPs have separated Nano spherical structures The size of ZnS 44 nm (48).

Fourier transforms infrared (FTIR) characterization

The FTIR technique was analyzed to determine functional groups and associations between chitosan and ZnS were investigated. The FTIR study revealed that the characteristic peaks of chitosan were at 1641cm-1 and 1645 cm-1, respectively, representing the amino group (NH2+) and amide I. Three bands of primary amine ranged between 3400 cm-1 and 3200 cm-1. (35). Peaks observed at 2947 cm-1, 1149 cm-1, and 1228 cm -1 were due to symmetric or asymmetric CH2 stretching vibration of pyranose ring and this was confirmed by (32). The N-H deformation band of chitosan was found at 1,564 cm-1 (19). Stretching vibrations of the C-H bond at 2308 cm-1 indicated the presence of aliphatic groups (52). The bands at1100-1000 cm-1 are due to the saccharide structure of the Chitosan (22). The FTIR spectrum of ZnS nanoparticles analysis was FTIR a spectrometer in a wavenumber range from 400 to 4000 cm−1 is shown in Figure 13. ZnS nanoparticles absorption peak observed at 657.73 and 613.36 cm−1 are assigned to the stretching modes of

ZnS (61). The bands exhibited from 3275.13 cm−1 and 3190.26 cm−1 are representing O-H of water molecules on the surface of nanoparticles (36). Moreover, N-H stretching of thiourea, whereas the vibration bands observed at 1683.86 cm−1 and 1429.25 cm−1 are the typical vibration bands of C = O and C-H (CH3) bending (55). The vibrational bands at 1203.58–1139.39 cm−1 are probably attributed to C-H stretching and the band at 979.84 assigned to C-H bending (34). The weak bands at 1089.70 and 1037.70 are probably attributed to C-O stretching. The peak at 480 cm−1 is assigned to NH2 symmetric stretching vibration (68).

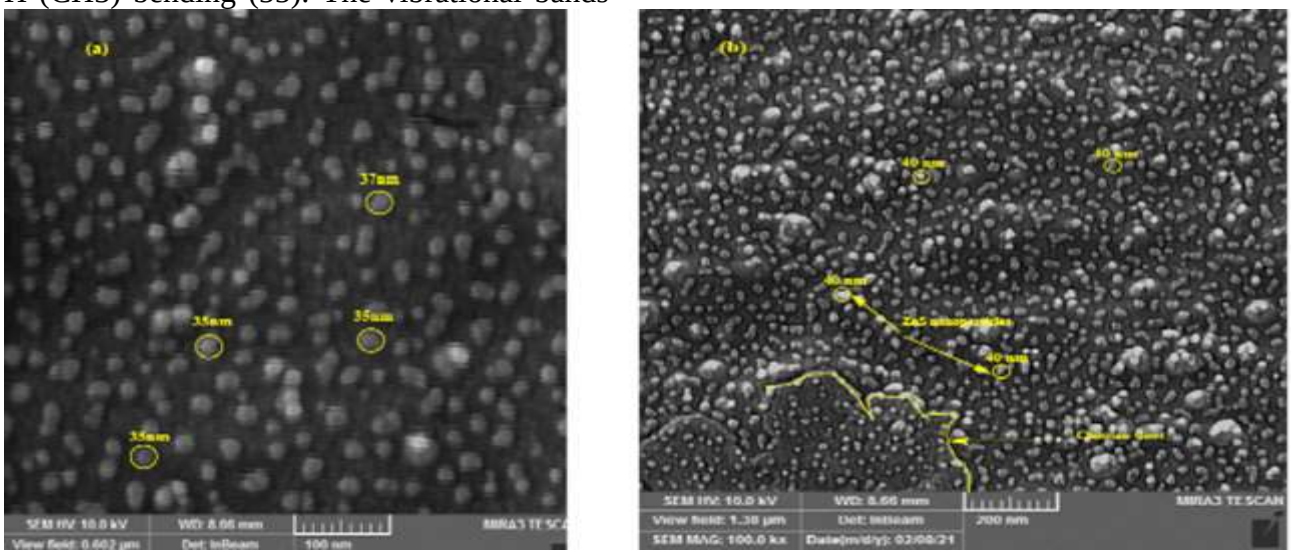

Figure 11. (FE-SEM) of Zinc sulfide chitosan nanoparticles

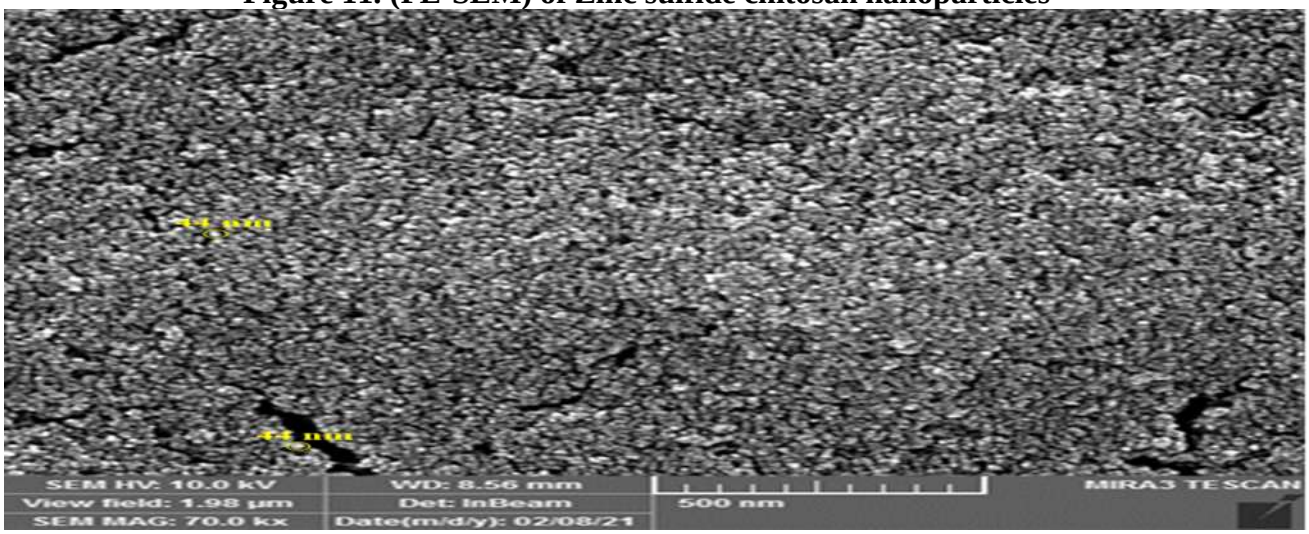

Figure 12. (FE-SEM) of Zinc sulfide nanoparticles

Represents the FT-IR spectra of the ZnS-chitosan composite. The efficient formation of ZnS-chitosan composite was shown by FT-IR Comparison of other composites. The bands, which were observed at 628 and 794 cm _1, are attributed to the stretching vibrations of the zinc-sulfur bond as shown in Figure 15. The Intensity of these peaks in composite decreased compared to that in ZnS due to the successful Formation of the composite (30). The wider band, which was observed at 3390 cm 1, is Owing to the stretching vibration of N-H or OH in chitosan as shown in Figure15. The band, Which was observed at 1408 cm _1, is owing to the stretching vibration of C = O which raised From the chitosan acetylated group as shown in Figure 14 .The band, which was observed at 1014 cm _1, is owing to the deformation of the CH3 group in chitosan as shown in figure 15. (31). these results, which were obtained in our work, are consistent with other papers by (1).

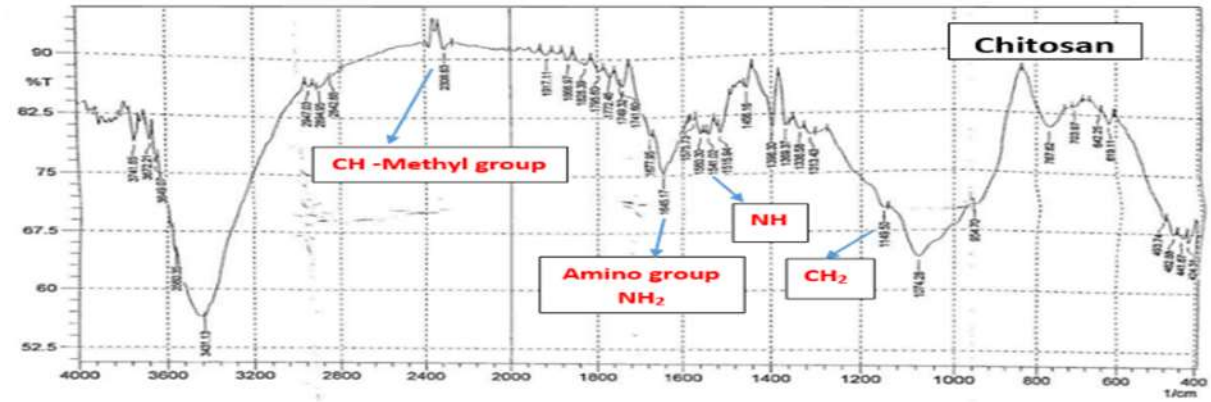

Figure 13.The Fourier Transforms Infrared (FT-IR) Spectroscopy Measurement of Chitosan

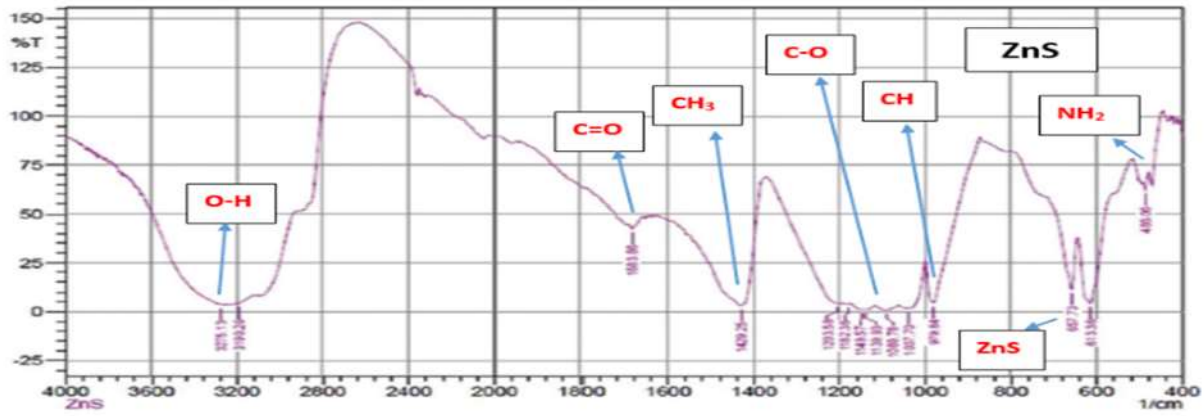

Figure 14. The Fourier Transforms Infrared (FT-IR) Spectroscopy Measurement of ZnS

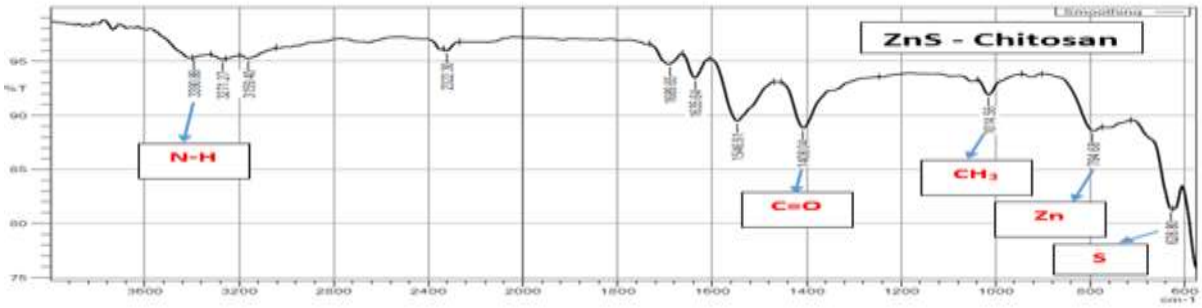

Figure 15. The Fourier Transforms Infrared (FT-IR) Spectroscopy Measurement of ZnS – Chitosan

Antibacterial susceptibility test

ZnS-chitosan nanoparticles were tested for antimicrobial activity against the multi-drug resistant gram-negative (*Pseudomonas aeruginosa*, *Acinetobacter baumannii* (and gram-positive (*Staphylococcus aureus*) bacteria that were selected for their extreme resistance to a variety of antibiotics. Many different concentrations of ZnS-chitosan were measured. (12.5, 25, 50, 100, 200 and 400 µg /ml). The results showed After 24 hrs of incubation under aerobic situation at 37 ºC, turbidity was seen in all test tubes containing *S. aureus* and ZnS-chitosan nanoparticles with a concentration (50, 100, 200, and 400 µg/ml). and the results were obtained for *Pseudomonas aeruginosa and A. baumanii* and ZnS-chitosan with a concentration (100, 200, and 400 µg/ml). The pathogenic bacterial strains demonstrated variable MIC50 µg/ml to 400 µg/ml for gram-positive bacteria and 100 to 400 µg/ml for gram-negative bacterial pathogens, respectively (Table 1). There was a significant effect on (*S.aureus)* bacteria than on both the *P.aeurginosa* and *A.baumanii* bacteria. These results agree with an early study that reported the stronger antibacterial effect of ZnS-chitosan on gram-positive

bacteria than gram-negative bacteria (56).In this study, ZnS-chitosan NPs showed remarkable antibacterial action against gram-positive and negative bacteria even at low concentrations as shown in Table (5). Based on the difference in the bacterial structure the activity of ZnS-chitosan on the gram-positive bacteria was more than its activity on gram-negative bacteria because the interaction between nanoparticles and cell surfaces would differ that lead to an effect on the penetrability of membranes since the entrance of nanoparticles inside bacterial cell induces oxidative stress consequently leading to inhibit cell growth and ultimately cell death (6).The mechanism of action of Zns nanoparticles was still unidentified; however, the predicted action that ZnS could adhere to the cell surface and cause damage to the cell membrane or they can electrostatically interact with the surface of the cell (21). Moreover, Chitosan is non-toxic, biodegradable, and biocompatible, and it is among the most popular bacteriostatic and bactericidal natural polymers with inherent antimicrobial activity (42). The demonstration of CH antibacterial activity on gram+ve bacteria is the non-covalent binding of chitosan to teichoic acid embedded into the peptidoglycan layer (51). The position of teichoic acid molecules on the surface is essential for the division of cells. Consequently, the interaction of CH could affect this operation and it can affect other operations which are very essential for bacterial Teichoic acids have the role of protecting cells from the stress of the environment, in order to control the activity of enzymes and ensure the cationic concentration of cell surface in order to promote cell binding to receptors. While its effect on gram-negative bacteria associated with chitosan's chelation interaction with cations when the pH above pKa (18).

Table 5. Minimum inhibitory concentrations of ZnS-chitosan nanoparticles on bacteria after 24 hrs. Incubation at 37 C

No.	ZnS-chitosan NPs concentration mg/	MIC		
		S. aureus	*P.aeruginosa*	*A. baumannii*
1	**400**	+	+	+
2	**200**	+	+	+
3	**100**	+	+	+
4	**50**	+	-	-
5	**25**	-	-	-
6	**12.5**	-	-	-

Cytotoxicity of ZnS-chitosan nanoparticles

The MTT assay was applied to determine the cytotoxic activity of the ZnS-chitosan NPs on normal (WRL- 68) cell lines. This assay has used a range of ZnS-chitosan NPs concentrations on normal cell lines ($1x10^{4}$ – $1x10^{6}$ cells / mL) to detect the cell viability. Results in Figure (16) showed that the dose-dependent manner of ZnS NPs caused a reduction in the cell viability of WRL 68 cell lines, in addition to measuring the IC50 of 156µg/ml. ZnS-chitosan NPs displayed a dose-dependent sequence of progressive cytotoxicity beginning at a lower concentration to its maximum inhibition at 400µg/mL,(15)% inhibition of WRL - 68 cells Evidence of the cytotoxic effect of ZnS-chitosan NPs revealed that treatment of WRL 68 cells at concentrations between (6.25) and (400) µg / mL for 24 hours showed cell viability mortality rate 2% by rising dose-dependent concentration reaching a death rate of up to 15% at (400) µg / mL with IC50 of (156) µg / mL (Figure16) and Table(6)

Table 6. ZnS-chitosan toxicity on WRL68 (X...ZnS-chitosan NPs concentration)

(X) concentration (µg/ml)	WRL68 Mean ± SD of viability (%)
400	
200	**93.63 ±1.45**
100	**94.28 ± 1.39**
50	**97.16 ±1.30**
25	**98.45 ±1.70**
12.5	**98.30 ±1.65**
LSD value	**8.177***

The synthesized ZnS-chitosan NPs demonstrated noticeable biocompatibility as is evident from the cytotoxicity (MTT) assay The tested ZnS-chitosan NPs (up to 400 µg/ml concentration) did not induce any significant cytotoxicity normal WRL 68 cells line even after 72 h of post-treatment, This is in agreement with the previous reports (25).

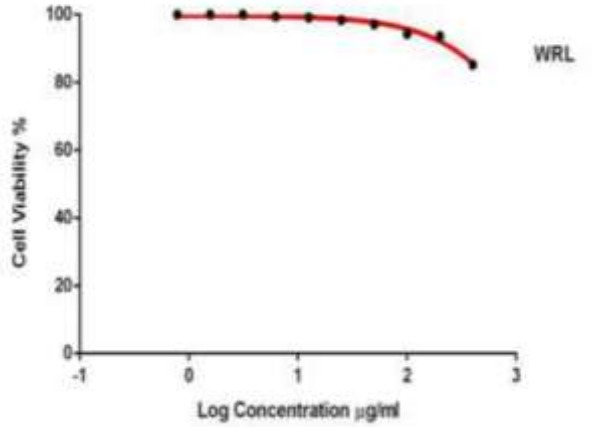

Figure 16. Cytotoxic activity of ZnS-chitosan NPs in a dose-dependent manner on WRL-68 cells at 37oC after 24hrs incubation

Conclusion: Direct functionalized chitosan to ZnS NPs were synthesized by using a modified single-step process at size 35nm with very good stability at pH 7, temperature 60℃, reaction time 60min, with 0.04 mg/ml of Zinc chloride, 2.5 ml 0.1mg/ml Sodium sulfide and 0.009 M chitosan. The results demonstrated that ZnS –Chitosan was more stable and showed a promising synergistic effect on gram-negative and positive bacteria than ZnS NPs

REFERENCES

1.Abdelrahman E.A., and R.M. Hegazey. 2019 Exploitation of Egyptian insecticide cans in the fabrication of Si/Fe nanostructures and their chitosan polymer composites for the removal of Ni(II), Cu(II), and Zn(II) ions from aqueous solutions, Compos. B Eng. 166 382–400

2.Aftab, S., M., M and A., Tarik,. M. Siddique, and M. A. Yusuf 2014. Clinical and microbiological aspect of wound infection: a review update. bangladesh Journal of Infectious Diseases, 1(2), 32-37

3.Al-Byti, A. M., S. A., Chakmakchy, A. A., Waheeb, and M. A. Alazzawy 2019. Study of isolated bacteria from burn wound of patients attended Plastic Surgery and Burns Unit. Indian Journal of Forensic Medicine and Toxicology, 13(4), 1462-1466

4.Alharbi, A., K., Shah, R. A., Sayqal, A., Subaihi, Alluhaybi, A. A., K., Algethami, F.... and M. H. Youssef, 2021. Facile synthesis of novel zinc sulfide/chitosan composite for efficient photocatalytic degradation of acid brown 5G and acid black 2BNG dyes. Alexandria Engineering Journal, 60(2), 2167-2178

5.Ali, H. I., H. A. Salih, and H. A. Al-jezani 2019. Preservative study of the AgNPs effect on the materials and embryonic development in albino rats. Iraqi Journal of Agricultural Sciences. 50(6): 1605-1612

6. Ali, A., M., Aadil, A., Rasheed, I., Hameed, S., Ajmal, I., Shakir, and M. F ,Warsi 2020. Honeycomb like architectures of the Mo doped ZnS@ Ni for high-performance asymmetric supercapacitors applications. Synthetic Metals, 265, 116408

7.Ali, Z. I., M., R., Mosallam, F. Sokary, Afify, A., T. & M. Bekhit, 2021. Radiation synthesis of ZnS/chitosan nanocomposites and its anti-bacterial activity. International Journal of Environmental Analytical Chemistry, 101(3), 379-390

8. Areekala, G. R., S., Fatahian, and N, Kianpour 2014. Investigation of ZnS nanoparticle antibacterial effect. Current Nanoscience, *10*(6), 796-800

9.Aynalem, M., E. S., Mengistu, G., Teklay, T., Moges, and M, Feleke 2017. Bacterial isolates and their antimicrobial susceptibility patterns of wound infections among inpatients and outpatients attending the University of Gondar Referral Hospital, Northwest Ethiopia. International Journal of Microbiology, 2017, 1-10

10.Baruah, J. M., S., Kalita, and J, Narayan 2019. Green chemistry synthesis of biocompatible ZnS quantum dots (QDs): their application as potential thin films and antibacterial agent. International Nano Letters, 9(2), 149-159

11.Biadglegne, F., B., Abera, A., Alem, and B. ,Anagaw, 2009. Bacterial isolates from wound infection and their antimicrobial susceptibility pattern in Felege Hiwot referral Hospital North West Ethiopia. Ethiopian Journal of Health Sciences, 19(3).

12.Bowman, K., and K. W., Leong 2006. Chitosan nanoparticles for oral drug and gene delivery. International journal of Nanomedicine, 1(2), 117

13.Cerqueira, G. C., A. M., Earl, C. M., Ernst, Y. H., Grad, J. P., Dekker, M., Feldgarden, and W. P. ,Hanage 2017. Multi-institute analysis of carbapenem resistance reveals remarkable diversity, unexplained mechanisms, and limited clonal outbreaks. Proceedings of the National Academy of Sciences, 114(5), 1135-1140

14.Clinical and Laboratory Standards Institute. 2018. Performance standards for antimicrobial susceptibility testing. 28th ed. CLSI supplement M100

15.Dryden, M.S. 2010 Complicated skin and soft tissue infection. Journal of Antimicrobial Chemotherapy, 65, 35-44.

16.Ergin, A. D., S., Bayindir, Z. and N. Yüksel 2019. Characterization and optimization of colon targeted S-adenosyl-L-methionine loaded chitosan nanoparticles. Marmara Pharmaceutical Journal, 23(5).

17.Farrag, H. A., A. H., El-Rehim, M. M., Hazaa, and A. S.,El-Sayed 2016. Prevalence of pathogenic bacterial isolates infecting wounds and their antibiotic sensitivity. Journal of Infectious Diseases and Treatment, 4, 5

18.Fu, B., Q., Wu, M., Dang, D., Bai, Q., Guo, L., Shen, and K.,Duan 2017. Inhibition of *Pseudomonas aeruginosa* biofilm formation by traditional chinese medicinal herb herba patriniae. Bio Med Research International, 28(5)1278-2198.

19.Gawad, R., and V.,Fellner 2019. Evaluation of glycerol encapsula ted with alginate and alginate-chitosan polymers in gut environment and its resistance to rumen microbial degradation. Asian-australasian Journal of Animal sciences, 32(1), 72

20.Guo, Y., K., X., Ruan, X., Shi, and Gu J. Yang, 2020. Factors affecting thermal conductivities of the polymers and polymer composites: A Review. Composites Science and Technology, 193, 108134

21.Hrebenyk, L. I., T. V., Ivakhniuk, and L. F.,Sukhodub. 2017. ZnS quantum dots encapsulated with alginate: Synthesis and antibacterial properties. In *IEEE* 7th International Conference Nanomaterials: Application & Properties (NAP) (pp. 04NB07-1). IEEE

22.Jaya, S., T. D., Durance, and R.,Wang 2010. Physical characterization of drug loaded microcapsules and controlled in vitro release study. the open Biomaterials Journal, 2(1).

23.Jayakumar, R., D., Menon, K.,Manzoor, S. V. , Nair, and H. ,Tamura2010. Biomedical applications of chitin and chitosan based nanomaterials a short review. Carbohydrate Polymers, 82(2): 227-232

24.Jayalakshmi, M. and M. M. Rao. 2006. Synthesis of zinc sulphide nanoparticles by thiourea hydrolysis and their characterization for electrochemical capacitor applications. J. Power Sources. 157: 624-629

25.Jayasree, A., S., Sasidharan, M., Koyakutty, S., Nair, and D.,Menon 2011. Mannosylated chitosan-zinc sulphide nanocrystals as fluorescent bioprobes for targeted cancer imaging. Carbohydrate Polymers, 85(1), 37-43

26.Jothimani, B., S., Sureshkumar, and B.,Venkatachalapathy 2017.Synthesis and characterization of surface modified, fluorescent and biocompatible ZnS nanoparticles with a hydrophobic chitosan derivative. Journal of Fluorescence, 27(4), 1277-1284

27.Kadhum and K.,Hussein 2020. Detection of the antimicrobial activity of silver nanoparticles biosynthesized by Streptococcus pyogenes bacteria. Iraqi journal of Agricultural Sciences, 51(2), 500-507

28.Kannan, S., N. P., Subiramaniyam, and M.,Sathishkumar 2020. A novel green synthesis approach for improved photocatalytic activity and antibacterial properties of zinc sulfide nanoparticles using plant extract of Acalypha indica and Tridax procumbens. Journal of Materials Science: Materials in Electronics, 31, 9846-9859

29.Katuwavila, N. P., L., Perera, A. D. R., Samarakoon, S., P., Soysa,. V., Karunaratne, A., Amaratunga, G. and D., Karunaratne,. 2016. Chitosan-alginate nanoparticle system efficiently delivers doxorubicin to MCF-7 cells. Journal of Nanomaterials, 2016

30.Khan, A., S., Badshah, and C.,Airoldi 2011. Dithiocarbamated chitosan as a potent biopolymer for toxic cation

remediation. Colloids and Surfaces B: Biointerfaces, 87(1), 88-95

31.Parvaneh, I., S., Samira, and N. ,Mohsen 2015. Characterization of ZnS nanoparticles synthesized by co-precipitation method. Chinese Physics B, 24(4), 046104

32.Kulig, D., A., Zimoch-Korzycka, A., Jarmoluk, and K.,Marycz 2016. Study on alginate–chitosan complex formed with different polymers ratio. Polymers, 8(5), 167

33.Kwamboka, B., W., Omwoyo, and N.,Oyaro 2016. Synthesis, characterization and antimicrobial activity of ZnS nanoparticles

34.Labiadh, H., K., Lahbib, S., Hidouri, S., Touil, and T. B. ,Chaabane 2016. Insight of ZnS nanoparticles contribution in different Biological uses. Asian Pacific Journal of tropical medicine, 9(8), 757-762

35.Lawrie, G., I., Keen, B., Drew, A., Chandler-Temple, L., Rintoul, P., Fredericks, and L. ,Grøndahl 2007. Interactions between alginate and chitosan biopolymers characterized using FTIR and XPS. Biomacromolecules, *8*(8), 2533-2541

36.Li, G., J., Zhai, D., Li, X., Fang, H., Jiang, Q., Dong, and E. ,Wang 2010. One-pot synthesis of monodispersed ZnS nanospheres with high antibacterial activity. Journal of Materials Chemistry, 20(41), 9215-9219

37.Li, S.; Y.; Shen, A.; Xie, X.; Yu, L.; Qiu, L., Zhang, and Q.,Zhang,.2007. Green synthesis of silver nanoparticles using *Capsicum annuum* L. extract. Green Chemistry, 9(8): 852-858

38.Liaqat, F. and R. Eltem, 2018. Chitooligosaccharides and their biological activities: a comprehensive review. Carbohydrate Polymers, 184: 243-259

39.Lyles, V. D., W. K., Serem, J. J., Yu, and J. C.,Garno 2013. Surface Characterization Using Atomic Force Microscopy (afm) in liquid environments. In Surface Science Techniques Springer, Berlin, Heidelberg(pp. 599-620).

40.Madhumathi, K., N. S., Binulal, H., Nagahama, H., Tamura, K. T., Shalumon, N. ,Selvamurugan, and R. ,Jayakumar 2009. preparation and characterization of novel β-chitin–hydroxyapatite composite membranes for tissue engineering applications. International Journal of Biological Macromolecules, 44(1): 1-5

41.Maryam, U. 2015. Isolation of pathogens causing sepsis, pus and infected wounds from critical care unit: a retrospective study. annals of clinical and laboratory Research, 3(4), 50

42. Matica, A., G., Menghiu, and V.,Ostafe 2017. Antibacterial properties of chitin and chitosans. New Frontiers in Chemistry, 26(1), 39-54.

43.Matsuura, Bader, M. S. 2008. Diabetic foot infection. American Family Physician, 78(1), 71-79

44.Mohammed, A., M. E., Seid, T., Gebrecherkos, M., Tiruneh, and F., Moges 2017. Bacterial isolates and their antimicrobial susceptibility patterns of wound infections among inpatients and outpatients attending the university of gondar referral hospital, Northwest ethiopia. International Journal of Microbiology, 98:425-132

45.Ohalete, C.N., R.K. Obi, and M.C., EmeaKoroha 2012. Bacteriology of different wound infection and their antimicrobial susceptibility patterns in imo state, Nigeria. World Journal of Pharmaceutical Sciences, 13, 1155-1172

46.Olayinka, A.T., B.A.,Onile, and B.O.,Olayinka 2004. Prevalence of multi-Drug resistant (MDR) pseudomonas aeruginosa isolates in surgical units of ahmadu bello university teaching hospital, zaria, nigeria: An Indication for effective control measures. Annals of African Medicine, 1, 13-16

47.Omole, A. and E. , Stephen 2014. Antibiogram profile of bacteria isolated from wound infection of patients in three hospitals in anyigba, kogi Sate, nigeria. FUTA Journal of Research in Sciences, 2, 258-266. omplex. Heliyon, 4(8), e00737

48.Othman, R. S., R. A., Omar, K. A., Omar, A. I., Gheni, R. Q., Ahmad, S. M., Salih, and A. N.,Hassan 2019. Synthesis of zinc sulfide nanoparticles by chemical coprecipitation Method and its bactericidal activity application. Polytechnic Journal, 9(2), 156-160

49.Patrulea, V., V., Ostafe, G.,Borchard, and O.,Jordan 2015. Chitosan as a starting material for wound healing applications. European Journal of Pharmaceutics and Biopharmaceutics, 97: 417-426

50.Pişki S.; A. ,Palantöken, and M. S. ,Yılmaz 2013. Antimicrobial activity of synthesized TiO2 nanoparticles. International Conference

on Emerging Trends in Engineering and Technology (ICETET'2013): 7-8

51.Raafat, D., and H. G., Sahl 2009. Chitosan and its antimicrobial potential–a critical literature survey. Microbial biotechnology, 2(2), 186-201

52.Raghu, S., and G., Pennathur 2018. Enhancing the stability of a carboxylesterase by entrapment in chitosan coated alginate beads. Turkish Journal of Biology, 42(4), 307-318

53.Ramanery, F. P., A. A., Mansur, and H. S. Mansur 2013. One-step colloidal synthesis of biocompatible water-soluble zns quantum dot/chitosan non conjugates. Nanoscale Research letters, 8(1), 1-13

54.Ramnani, S. P., J., Biswal, and Sabharwal, S. 2007. Synthesis of silver nanoparticles supported on silica aerogel using gamma radiolysis. Radiation Physics and Chemistry, 76(8-9), 1290-1294.

55.Reddy, D. A., C., Liu, R. P., Vijayalakshmi, and B. K. ,Reddy 2014. Effect of Al doping on the structural, optical and photoluminescence properties of ZnS nanoparticles. Journal of Alloys and Compounds, 582, 257-264

56.Sahu, B.K. 2013. Antimicrobial properties of Aerial Part of Sesbaniagrandiflora (Linn.), The Pharmaceutical College Barpali, India

57.Sahu, S., J.,Shergill, P. Sachan, and R Gupta,. 2011. Superficial incisional surgical-site infection in elective abdominal surgeries—a prospective study. The Internet Journal of Surgery, 26, 514-524.

58.Salehizadeh, H., E., Hekmatian, M., Sadeghi, and K.,Kennedy 2012. Synthesis and characterization of core-shell Fe 3 O 4-gold-chitosan Nanostructure. Journal of Nanobiotechnology, 10(1), 1-7

59.Sani, R.A., S.A.,Garba, and O.A.,Oyewole 2012. Antibiotic resistance profile of gram-negative bacteria isolated from surgical wounds in minna, bida, kontagora and suleja areas of Niger State. American Journal of Medicine and Medical Sciences, 2, 20-24

60.Saranya, N., A., S., Moorthi, M. Saravanan, P. Devi, and N. Selvamurugan 2011. Chitosan and its derivatives for gene delivery. International Journal of Biological Macromolecules, 48(2): 234-238.

61.Senapati, U. S., D. K., Jha, and D. ,Sarkar 2013. Green synthesis and characterization of ZnS nanoparticles. Research Journal of Physical Sciences ISSN, 2320, 4796

62. Shaban, S. M. 2016. Studying the effect of newly synthesized cationic surfactanton silver nanoparticles formation and their biological activity. Journal of Molecular Liquids, 216, 137-145

63.Siddiqui, A.R. and J.M.,Bernstein 2010. Chronic wound infection: facts and controversies. Clinics in dermatology, 28, 519-526

64.Sreekala G. N., F., Abdullakutty B., Beena 2019. Green synthesis, characterization and photo catalytic degradation efficiency of trimanganese tetroxide nanoparticle. Int. J. Nano Dimens. 10: 400-409

65.Tessema, A. 2017. Antimicrobial susceptibility pattern of bacterial isolates from wound infections at all Africa leprosy, tuberculosis and rehabilitation training center, addis ababa Ethiopia

66.Tom, I. M. 2019. Infection of wounds by Potential bacterial pathogens and their resistogram. Open Access Library Journal, 6(07), 1

67.Traisaeng, S., D. R., Herr, H. J., Kao, T. H., Chuang, and C. M.,Huang 2019. A derivative of butyric acid, the fermentation metabolite of staphylococcus epidermidis, inhibits the growth of a staphylococcus aureus strain isolated from atopic dermatitis patients. Toxins, *11*(6), 311

68.Wageh, S., Z. S., Ling, and Xu- X. ,Rong 2003. Growth and optical properties of colloidal ZnS nanoparticles. Journal of Crystal Growth, 255(3-4), 332-337

69.Wang, S., D., Yu, G., Wu, J., Guo, and C.,Lei 2011. A new fluorescent film sensor for Pb (II) ions developed by simulating bio-mineralization process synthesizing of ZnS/CS nanocomposite. Materials Science and Engineering: B, 176(12), 873-877

70.Ye, Y., L., Xu, Y., Han, Z., Chen, C., Liu, and L.,Ming 2018. Mechanism for carbapenem resistance of clinical enterobacteriaceae isolates. Experimental and Therapeutic Medicine, *15*(1), 1143-1149

71.Yonis and *et al.*, 2019. Statistical Optimization of Chitin Bioconversion to Produce AN Effective Chitosan in Sold State

Fermentation by Asperigellus flavus. Iraqi Journal of Agricultural Sciences, 50(3).
72.Younes, I. 2015. Rinaudo M. Chitin and cs preparation from marine sources. Structure, properties and applications. Mar. Drugs, 13(3): 1133-1174
73.Yuan, G., X. Chen, and, D., Li, 2016. Chitosan films and coatings containing essential oils: The antioxidant and antimicrobial activity, and application in food systems. Food Research International, 89: 117-128.